Desalination and Water Treatment
www.deswater.com

doi:10.5004/dwt.2019.24456

164 (2019) 151–161
October

Underwater superoleophobic porous hydrogel film prepared by soluble salt-template method for oil/water separation in complex environments

Zhongxin Xue[a,*], Xiaowei Xing[a], Shuxu Zhu[a], Wei Zhang[a], Liying Luan[b], Yuzhong Niu[a], Liangjiu Bai[a], Hou Chen[a], Qian Tao[a]

[a]*School of Chemistry and Materials Science, Ludong University, Yantai, 264025, China, email: ldxuezx@126.com (Z. Xue), 823573697@qq.com (X. Xing), 17862823153@163.com (S. Zhu), zw921656296@163.com (W. Zhang) niuyuzhong@126.com (Y. Niu), bailiangjiu@163.com (L. Bai), ldupolymchen@163.com (H. Chen), amytaoqian@126.com (Q. Tao)*
[b]*School of Life Sciences, Ludong University, Yantai, 264025, China, email: luanliying@163.com (L. Luan)*

Received 30 January 2019; Accepted 22 May 2019

ABSTRACT

A porous calcium alginate/Ag nanoparticles (Ca-ALG/Ag) hydrogel film with superhydrophilic and underwater superoleophobic properties is fabricated through an eco-friendly "soluble salt-template method". Taking advantage of the environmental stability of calcium alginate and the freestanding porous structures, the Ca-ALG/Ag hydrogel film can selectively and effectively separate oil/water mixtures in highly acidic, alkaline, and salty environments. The introduction of Ag nanoparticles enhances the superoleophobicity, also provides antibacterial activities against *Escherichia coli* (Gram negative bacterium) and *Staphylococcus aureus* (Gram positive bacterium). This Ca-ALG/Ag hydrogel film is stable, antibacterial, eco-friendly and reusable, which shows potential use for oil spill cleanup and oily wastewater treatment in practical complex environments. Furthermore, the "soluble salt-template method" brings a new strategy to prepare other hydrogel films with macro-porous structures for oil/water separation.

Keywords: Underwater superoleophobicity; Oil/water separation; Hydrogel; Template method; Alginate

1. Introduction

Recently, large amount of oily wastewater discharged from our daily life and industries such as steel, food, textile, leather, petrochemical and metal finishing, has caused serious environmental problems [1–3]. In addition, frequent oil spill accidents have released millions tons of crude oil to seas and rivers, threatening the environmental system and leading to a waste of resources [4,5]. The environmental and economic demands highlight the urgent need for functional materials that can separate oil/water mixtures efficiently. Since oil/water separation is an interfacial issue, designing novel materials with special wettability is an effective strategy [6–11]. In the past few years, there is an explosion in the development of various materials based on this strategy, which can be generally categorized into "oil-removing" type and "water-removing" type [7–9]. The "oil-removing" type of materials can selectively filtrate or absorb oil from oil/water mixtures due to their superhydrophobic and superoleophilic properties. This type of material is effective especially in emergency management of oil spill accidents [7,12–14]. However, the "oil-removing" type of materials can be easily fouled or even blocked by oils due to their oleophilic property, which significantly decrease the separation capacity and limits the recycle times.

In recent years, the "water-removing" type of materials has aroused wide attention for their superhydrophilic and underwater superoleophobic properties [15–21]. The superoleophobicity protects materials from fouling by oils, and thus can essentially overcome aforementioned problems, which gives them better performance in recycling of oil and reuse of materials. However, there are still some limitations.

*Corresponding author.

Most of the materials are fabricated by combining special wettable coatings with porous substrates, such as stainless steel mesh, copper grid, polymer fabrics, etc [8,17,22]. The coating may shed off from the substrate after using for long time, thus lost the separation capacity. Moreover, the decomposing and corroding of metal substrates in acidic, alkaline or salty solutions limit the application in complex environments. Furthermore, the disposal of used materials remains as a challenging task, because most of the materials are non-degradable in natural environment. So far, the common treatment approaches are directly discarded or burnt, which will cause soil contaminants and noxious gases, accordingly resulting in secondary pollution. In addition, there are a large number of pathogenic bacteria, viruses and micro-organisms in practical oily wastewater, which make a serious threat to the nature environment and human health [1]. Nevertheless, the "water-removing" type of separation materials with antibacterial properties is rarely reported. Therefore, it is significant to develop separation materials that are stable in highly acidic, alkaline or salty solutions, eco-friendly and antibacterial for application in practical complex environments.

Nature offers an inspiration to develop such multifunctional materials. The surface of the seaweed Saccharina japonica is covered with polysaccharides that exhibit underwater superoleophobicity and antibiofouling behavior in highly acidic, alkaline or salty environments [23]. Alginate, which is the main component of the seaweed, is a linear, unbranched polysaccharide composed of repeating (1,4)-linked β-D-mannuronic and α-l-guluronic acid. Alginate can crosslink with polyvalent metal cations like Ca^{2+} to produce strong hydrogels [24–29]. It is a renewable and environmentally benign bioresource. Its low-cost, non-toxicity, good biocompatibility and biodegrability make it ideal for fabrication of multifunctional separation materials [30,31]. Moreover, the crosslinked network structures of alginate hydrogel are propitious to load antibacterial materials [32–34]. To improve the stability in complex solution environments, fabrication of free-standing porous hydrogel film without other substrates is an effective way. So far, template method is a common technique to prepare macro-porous hydrogel films. In general, the templates are insoluble in water but soluble in acidic or alkaline solutions, such as $CaCO_3$ and silica particles [35,36], which have to be leached out after the film gelation. The template-leaching process consumes a large amount of acid or alkali solutions, which will cause environmental pollution and make scale-up difficult. New preparation methods are needed to be developed.

In this work, through an eco-friendly "soluble salt-template method", we report the fabrication of a porous calcium alginate/Ag nanoparticles (Ca-ALG/Ag) hydrogel film with superhydrophilic and underwater superoleophobic properties. Taking advantage of the environmental stability of calcium alginate and freestanding porous structures, the Ca-ALG/Ag hydrogel film can selectively and effectively separate oil/water mixtures in highly acidic, alkaline, and salty environments. The Ag nanoparticles embedded in the film enhance the superoleophobicity, also provide antibacterial activities against *Escherichia coli* (Gram negative bacterium) and *Staphylococcus aureus* (Gram positive bacterium). This Ca-ALG/Ag hydrogel film is stable, antibacterial, eco-friendly and reusable, which shows potential use for oil spill cleanup and oily wastewater treatment in practical complex environments.

2. Experimental

2.1. Materials

Sodium alginate, calcium chloride, silver nitrate, sodium chloride, ascorbic acid were of analytical reagent grade and obtained from Sinopharm Chemical Reagent Co., Ltd., China. Crude Oil was kindly provided from the China Petroleum and Petrochemical Research Institute. Sea water was collected from the Yantai sea area.

2.2. Preparation of the porous Ca-ALG/Ag hydrogel films

The Ca-ALG hydrogel film with macro-porous structures was fabricated by combining ionic cross-linking and soluble salt-template method. The Ca-ALG/Ag hydrogel film was fabricated through incorporating Ag nanoparticles into alginate matrix by a simple reduction process [30] as described in Fig. 1. The Sodium alginate (ALG) was dissolved in deionized water and stirred for 2 h at 60°C to form a transparent solution (3 wt.%). Then the solution was spin-casted on clean glass slides at 500 rpm for 5 s and 1000 rpm for 30 s. NaCl crystals were chosen as templates, which were grinded by a mortar and then sieved by standard sieves with different pore sizes (150–180 μm, 100–150 μm and 75–100 μm). The mass ratio of NaCl templates and the ALG solution is 0.5:1. The NaCl templates were sifted on the ALG solution films. Then the ALG/NaCl composites were quickly immersed in $CaCl_2$ solution (5 wt.%) for 30 min, which was sonicated at the same time. During this step, three processes happened simultaneously: (i) NaCl crystals penetrated the film by ultrasonic concussion; (ii) NaCl crystals dissolved in $CaCl_2$ solution; and (iii) ionic crosslinking of ALG. The $CaCl_2$ immersion combined with ultrasonic treatment led to ionic crosslinking of ALG, dissolution of the NaCl templates and, consequently, the formation of insoluble films with macro-pore structures. Then, the as-prepared porous Ca-ALG hydrogel film was immersed in a 0.1 M $AgNO_3$ solution for 1 h, then rinsed with deionized water, and dried in a nitrogen flow. The loaded film was treated with a 0.1 M solution of ascorbic acid (pH = 4) for 1 h to reduce the silver salt to metallic nanoparticles.

2.3. Oil/water separation experiment

The as-prepared porous Ca-ALG hydrogel film was fixed between two glass tubes. The volume of upper tube was 300 mL while the below conical flask was 250 mL. Before the separation, the film was firstly wetted by water. Then the oil/water mixture (V_{water}/V_{oil} = 1:1) was poured into the upper tube. The separation process was achieved by the weight of the liquids. Flux was calculated based on the water quantity permeating through the films.

2.4. Antimicrobial activity experiment

We determined the antibacterial property of the Ca-ALG/Ag hydrogel film towards cultures of *Escherichia*

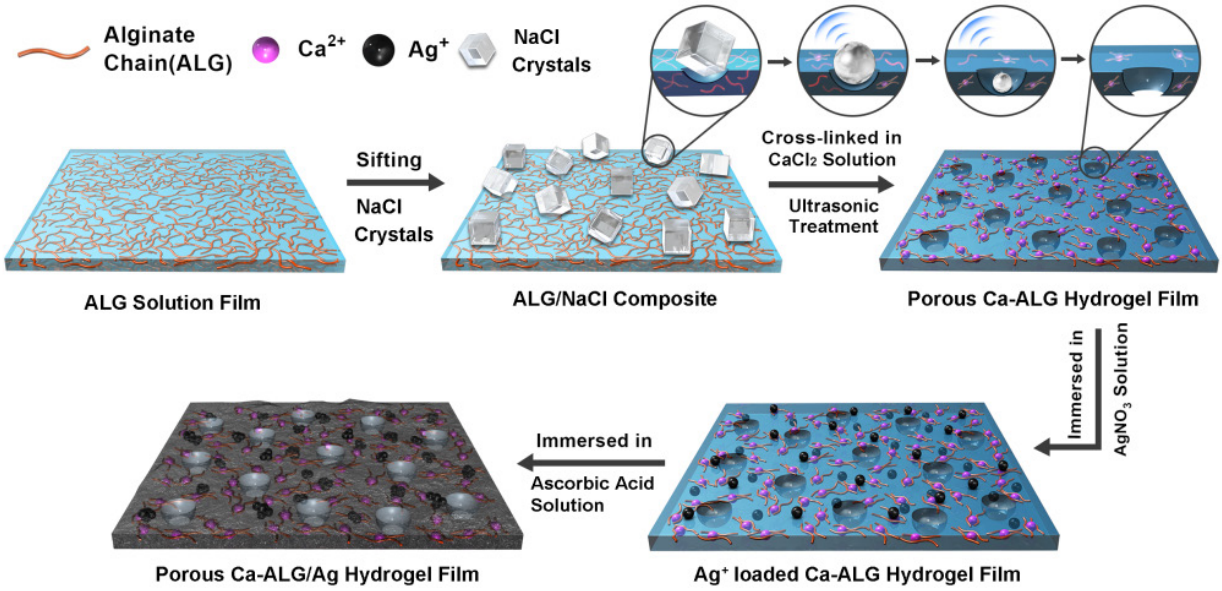

Fig. 1. Schematic description of the preparation of the porous Ca-ALG/Ag hydrogel film.

coli (Gram negative bacterium) and *Staphylococcus aureus* (gram positive bacterium). Lawns of *E. coli* and *S. aureus* were established on Luria-Bertani (LB) agar plates. The Ca-ALG/Ag and Ca-ALG hydrogel films were exposed to UV light for 30 s for sterilization purposes. The samples were placed on the bacteria lawns: one sample of Ca-ALG/Ag hydrogel film (with Ag nanoparticles) and one sample of Ca-ALG hydrogel film (without Ag nanoparticles). The size of the samples is 1×1 cm. The agar plates were incubated for 24 h at 37°C. The zones of inhibition are clearly seen on the photographs in Fig. 6. Five parallel experiments were carried out. Their sizes were measured using a ruler and presented as mean values.

The antimicrobial effect of Ca-ALG/Ag hydrogel film was also evaluated by the colony-counting method. A diluted *E. coli* suspension at about 1.0×10^6 colony forming units per milliliter (cfu/mL) concentration was prepared. 200 µL *E. coli* suspension was loaded onto the surface of the Ca-ALG/Ag hydrogel film piece (1×1 cm), and the inoculum on the surface was then carefully covered with another sterilized cover film in a sterilized glass-surface vessel before it was placed in an incubator at 37°C and relative humidity > 90%. Make sure the *E. coli* suspension did not leak beyond the edges of the membranes. After 24 h, the whole *E. coli* suspension was collected and serially diluted with sterilized water. 100 µL dilution was spread on LB agar plate which is prepared by dissolving 1 wt.% bacto-tryptone, 0.5 wt.% yeast extract, 1 wt.% NaCl, and 1.5 wt.% agar in sterilized water. The same procedure was also applied to the Ca-ALG hydrogel film piece as a blank control and the vessel (without any other materials) as a negative control. Viable bacterial colonies were counted after incubation at 37°C for 24 h. The reduction rate in the number of bacteria was calculated using the following expression [37,38]:

$$R = \frac{(B - A)\times 100}{B} \quad (1)$$

where R is the antibacterial efficiency of the corresponding sample, B and A are the number of colonies corresponding to the blank control sample and the antibacterial sample, respectively. Five parallel experiments were carried out. The antibacterial activity for *S. aureus* was obtained by the same process.

2.5. Instruments and characterization

Scanning electron microscopy (SEM) images were obtained by a field-emission scanning electron microscope (SU-8010, Hitachi Limited, Japan). The chemical composition was measured by energy dispersive spectroscopy (EDS, X-Flash6/60, Bruker). The porosity was the statistics of different pores in large scale. The contact angles and sliding angles were investigated on a contact angle meter (JC 2000, Shanghai Zhongchen Digital Technology Apparatus Co., Ltd.). For water and oil contact angle measurement in air, liquid droplets were directly put on the film. For underwater oil wetting performance measurement, the substrates were firstly fixed in a quartzose container and full of water. For 1, 2-dichloroethane with higher density than water, the oil droplet was directly put on the film. For oils with lower density than water, such as crude oil, the oil droplet was released under the film through an inverted needle. The average values were achieved by examining five points on the identical film. The rolling angles were investigated by tilting the film with a droplet (5 µL) that contact with the film until the droplet started to slide. Photographs in Figures were obtained on a camera (Canon 550D). The oil concentration of the original oil/water mixtures and the collected water after separation was measured by the infrared spectrometer oil content analyzer (OIL 480, China). CCl_4 was used to extract oils from water. The absorbance at 2930 cm^{-1}, 2960 cm^{-1}, and 3030 cm^{-1} were measured. The oil content was obtained by calculating the absorbance and the correction coefficient.

3. Results and discussion

In order to improve the traditional template-method, a simple "soluble salt-template method" was adopted innovatively. NaCl crystals were used as templates, which can be easily removed by water. After the NaCl templates were sifted on ALG solution films, the ALG/NaCl composites were quickly immersed in $CaCl_2$ solution, which was sonicated at the same time. During the Ca^{2+} crosslinking process, the NaCl crystals pierced through the ALG film and dissolved in water gradually, which generated macro-pore structures (Fig. 1). This strategy combined gelation and template-leaching process into one step. No other acidic or alkaline solution is needed to dissolve the templates. This one-step fabrication of porous Ca-ALG hydrogel film is exceedingly simple, low-cost, eco-friendly, and easily scale-up.

The as-prepared Ca-ALG hydrogel film is transparent with thickness of approximately 45 μm under swelling balance (Fig. 2a). Figs. 2b–d show the scanning electron microscopy (SEM) images of the Ca-ALG hydrogel film. Fig. 1b is a typical large-scale view of the Ca-ALG hydrogel film with an average pore size of 95.2 ± 21.7 μm. The pores distribute uniformly, which size can be controlled by selection of different sizes of NaCl templates. (See details in Experimental Section and Supporting Information Fig. S1). The enlarged view of a single pore (Fig. 2c) shows trumpet-shaped pore structure, owing to the gradual dissolution of NaCl templates. The higher magnification image of the Ca-ALG hydrogel film shows a smooth surface (Fig. 2d).

In order to increase the roughness of the surface and achieve antibacterial property, silver nanoparticles were synthesized inside the Ca-ALG hydrogel film. A simple ionic reduction process was adopted (See details in Experimental Section and Fig. 1). The presence of the Ag nanoparticles can be detected byEDS (Supporting Information Fig. S2). The load of the Ag is approximately 5~6 wt.%. Owing to the formation of embedded Ag nanoparticles, the as-prepared porous Ca-ALG/Ag hydrogel film becomes black and shows metallic luster under the light (Fig. 2e). The macro-porous structures and pore size remain unchanged before and after Ag nanoparticles embedded (Figs. 2f, 2d). The pore can also be clearly observed from the cross-sectional SEM image (Supporting Information Fig. S3). The higher-magnification SEM image of the porous Ca-ALG/Ag hydrogel film shows a rough surface with nanostructures. Random embedded nanoparticles with size of 400–650 nm can be clearly observed. The roughness of the Ca-ALG and Ca-ALG/Aghydrogel film is approximately 1.09 and 1.38 respectively (See details in Supporting Information). The rougher structures can amplify the surface wetting performance as reported [39,40]. It is expected that particular wetting performances can be observed on the Ca-ALG/Ag hydrogel film.

The wetting properties of the obtained films were investigated comprehensively by using a contact angle measure meter. In air, the porous Ca-ALG/Ag film shows superhydrophilic and superoleophilic properties (Fig. 3a and Table S1 in the Supporting Information). After immersion into water, as shown in Fig. 3b, an oil droplet (3 μL, 1, 2-dichloroethane) can stand on the film with a contact angle of about 161°, indicating that the film is underwater superoleophobic. To further study the wetting change between the Ca-ALG hydrogel films with and without Ag nanoparticles, the underwater OCAs of Ca-ALG and Ca-ALG/Ag hydrogel films for a series of oil droplets were measured comprehensively (Fig. 3c). The typical photographs of the oil droplets are shown as insets on the right in Fig. 3c. Compared to the Ca-ALG hydrogel film with OCAs of about 150°, the OCAs of Ca-ALG/Ag hydrogel film increase obviously, which are all above 160°. The underwater superoleophobicity becomes stronger due to the efforts of Ag with high surface energy and the hierarchical micro/nano structures. Meanwhile, the film shows low adhesion to the oil droplet which can roll away from the film with an extremely low sliding angle (less than 5°, Supporting Information Fig. S4).

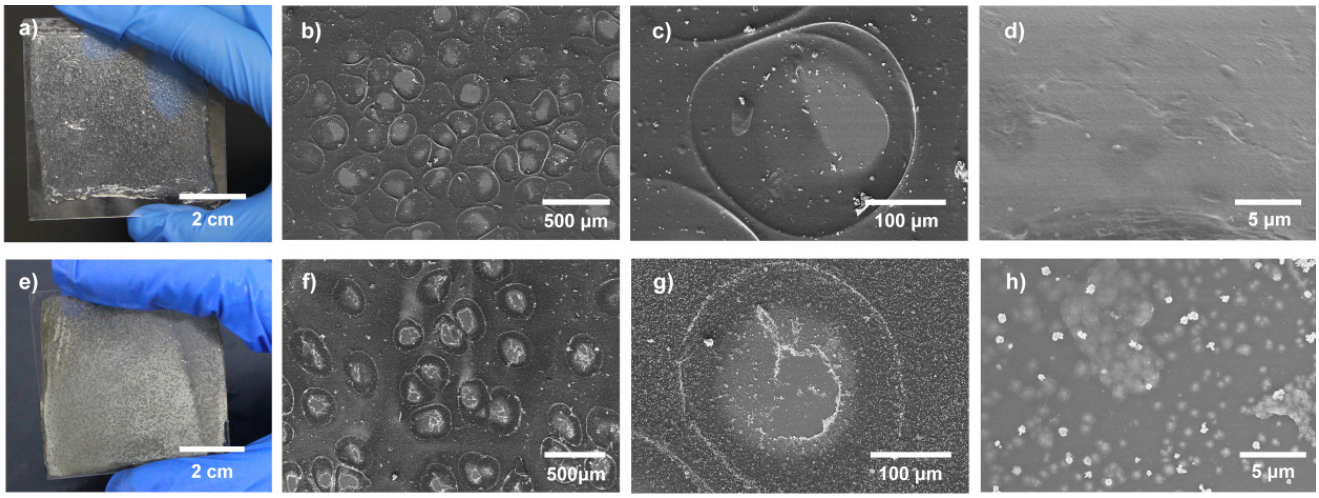

Fig. 2. Photographs and SEM images of the porous Ca-ALG hydrogel films with and without Ag nanoparticles. a) The photograph of the porous Ca-ALG hydrogel film. b) Large-area view, c) enlarged view of a single pore and d) higher-magnification SEM images of the porous Ca-ALG hydrogel film. e) The photograph of porous Ca-ALG/Ag hydrogel film. f) Large-area view, g) enlarged view of a single pore and h) higher-magnification SEM images of the porous Ca-ALG/Ag hydrogel film, in which the embedded Ag nanoparticles can be clearly observed.

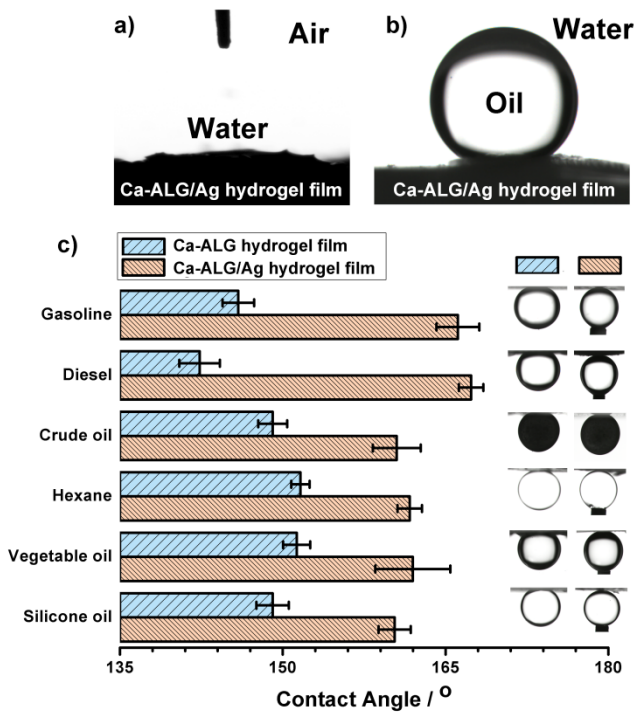

Fig. 3. The as-prepared Ca-ALG/Ag hydrogel film shows superhydrophilic and underwater superoleophobic properties. a) Photograph of a water droplet (3 μL) on Ca-ALG/Ag hydrogel film in air. b) Photograph of an oil droplet (DCE, 3 μL) on Ca-ALG/Ag hydrogel film in water. c) OCAs in water of Ca-ALG and Ca-ALG/Ag hydrogel films. The inserts are the representative photographs of oil droplets on Ca-ALG (left) and Ca-ALG/Ag (right) hydrogel films in water.

In order to further examine the oil-repellent ability of the film, an oil droplet was used to contact the film and then allowed to leave. Even the oil droplet was squeezed against the surface with the maximum preload that the system can supply, the oil droplet still left the film easily without any residual (Supporting Information Fig. S5), indicating that the Ca-ALG/Ag hydrogel film has an ultralow oil-adhesion property.

Taking advantage of the superhydrophilic/underwater superoleophobic properties and the porous structures of the Ca-ALG/Ag hydrogel film, a series of oil–water separation experiments were carried out. The separating process is displayed in Fig. 4. The Ca-ALG/Ag hydrogel film were pre-wetted with water in advance, and then fixed between two glass tubes. The mixture of crude oil and water was poured into the upper tube. It can be seen that without external force, water quickly permeated through the film and dropped into the beaker below due to the superhydrophilicity of the film. Meanwhile, crude oil was retained above the film because of the underwater superoleophobic property (Figs. 4a, b). These results indicate that using the as-prepared film, oil/water mixture can be separated easily. Other mixtures of water and oils, including gasoline, diesel, hexane, vegetable oil and silicone oil, were also investigated. All these mixtures can be separated successfully, indicating that the as-prepared film will have a wide range of applications.

To determine the separation efficiency, the oil contents before and after separation were measured on the infrared spectrometer oil content analyzer. The oil contents after separation was shown in Supporting Information Fig. S6. The separation efficiency can be obtained according to the following equation [17,41]:

$$R = \left(1 - \frac{C_P}{C_0}\right) \times 100\% \quad (2)$$

where C_o and C_p are the oil concentration of the original oil/water mixture and the collected water after one time separation, respectively. As shown in Fig. 4c, the separation efficiency of the Ca-ALG/Ag hydrogel film for a selection of oils was all above 98%. The flux was also calculated based on the water quantity permeating through the films within the calculated time. Flux rates of the Ca-ALG/Ag hydrogel film are 3200–4000 $L \cdot m^{-2} \cdot h^{-1}$ for the above oil/water mixtures (Fig. 4c). The ultrafast flux is attributed to the macro-porous structures and superhydrophilicity of the film. Furthermore, after separation, the film can be cleaned easily for reuse. Taking the diesel/water mixture as an example, the separation efficiency declined less than 0.1% after 40 cycles. The flux declined 5.9% after 20 cycles and 17.1% after 40 cycles. The separation efficiency and flux still maintains a relatively high level (Fig. 4d). The as-prepared Ca-ALG/Ag hydrogel film shows good stability and recyclability.

In practical applications, the environmental stability of the separating film is important. As for these "water-removal" type materials, because water will contact with these films intimately during the separating process, the stability of the film to corrosive liquid such as strong acid, strong basic and hypersaline water solution is crucial. Noticeably, the Ca-ALG/Ag hydrogel film in this work has such particular anti-corrosive ability, which originates from its rich content of polysaccharides and stability of three-dimensional interconnected network structure. To evaluate the anti-corrosive ability, the film was firstly immersed into aqueous solution with certain conditions (acid, basic or salt solutions) for about 24 h, and then oil wetting performances and separation efficiency of the film were examined. It can be seen that for all these water solutions, the underwater superhydrophobicity and low oil adhesions can still be present (Fig. 5a), and corresponding separating efficiency retains higher than 99% (Fig. 5b). The high separation efficiency of the Ca-ALG/Ag hydrogel film under acidic, alkaline, and salty conditions indicates its possible use for oil spill accidents in seawater or separation of industrial wastewater.

There are large quantities of pathogenic bacteria, viruses and micro-organisms in oily wastewater, which make a serious threat to the nature environment and human health [1]. In addition, the polysaccharides are easy to breed bacteria,such as alginate and agar. This is one of the biggest limitations for polysaccharides used in the field of oil-water separation. Therefore, for the practical application, antimicrobial is an important property. The introduction of anti-bacterial silver nanoparticles is an effective way to enhance practicability. The stored silver nanoparticles release silver ions and, with this mechanism, enhance antimicrobial function [37,42]. We studied the toxicity of the porous Ca-ALG/Ag and Ca-ALG hydrogel films to *Escherichia coli* (Gram negative bacterium) and *Staphylococcus aureus* (Gram positive bacterium). The

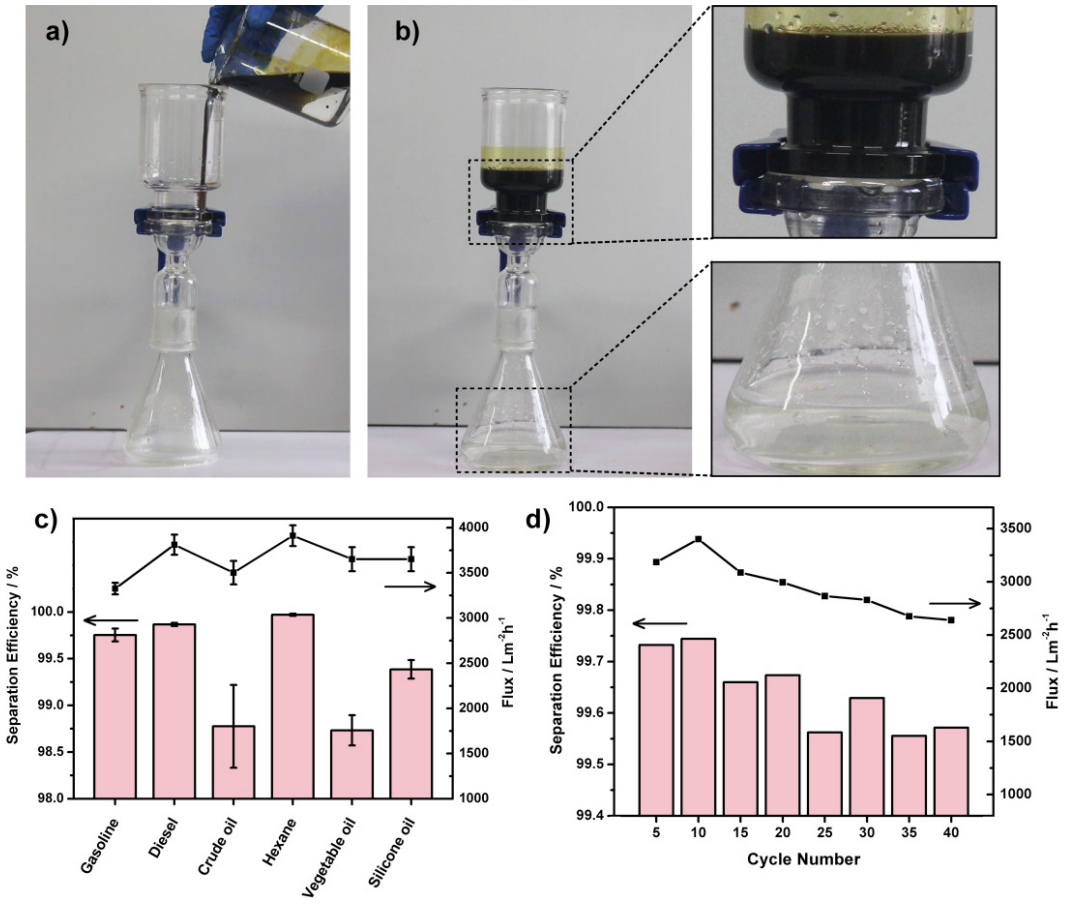

Fig. 4. Oil/water separation studies of the Ca-ALG/Ag hydrogel film. The pore size of the film is 95.2 ± 21.7 μm. a) The coated mesh was fixed between two glass tubes, the mixture of crude oil and water was put into the upper glass tube. b) Water selectively permeated through the Ca-ALG/Ag hydrogel film, while the oil was repelled and kept in the upper glass tube. c) The separation efficiency and flux of the Ca-ALG/Ag hydrogel film for a selection of oils. d) The separation efficiency and flux of diesel–water (V_{diesel}/V_{water} = 1:1) mixtures after 40 cycles. The separation efficiency declined less than 0.1% after 40 cycles.

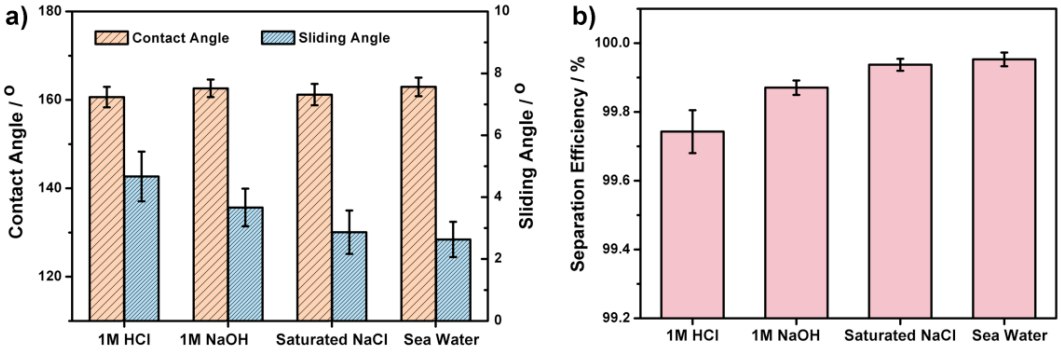

Fig. 5. The Ca-ALG/Ag hydrogel film exhibits superoleophobic property and stable separation ability in 1 M HCl, 1 M NaOH, saturated NaCl solution and sea water, respectively. a) Oil contact angles and sliding angles (DCE, 3 μL) on the Ca-ALG/Ag hydrogel film in the above corrosive liquids. b) The separation efficiency of the Ca-ALG/Ag hydrogel film for hexane in different solutions in terms of their oil rejection coefficient.

results (Fig. 6) clearly show that the Ca-ALG/Ag hydrogel film was inhibitory and bactericidal for the test organisms. The zones of inhibition were 2.1 ± 0.2 mm for *E. coli* and 1.02 ± 0.05 mm for *S. aureus*, whereas no inhibition zone appeared for Ca-ALG hydrogel film. The antimicrobial effect of the Ca-ALG/Ag hydrogel film was also evaluated by the colony-counting method (See details in Experimental Section and Supporting Information Fig. S7). The antibacterial efficiency of the Ca-ALG/Ag hydrogel film is 100% for *E. coli* and 99.25 ± 0.55% for *S. aureus*. These

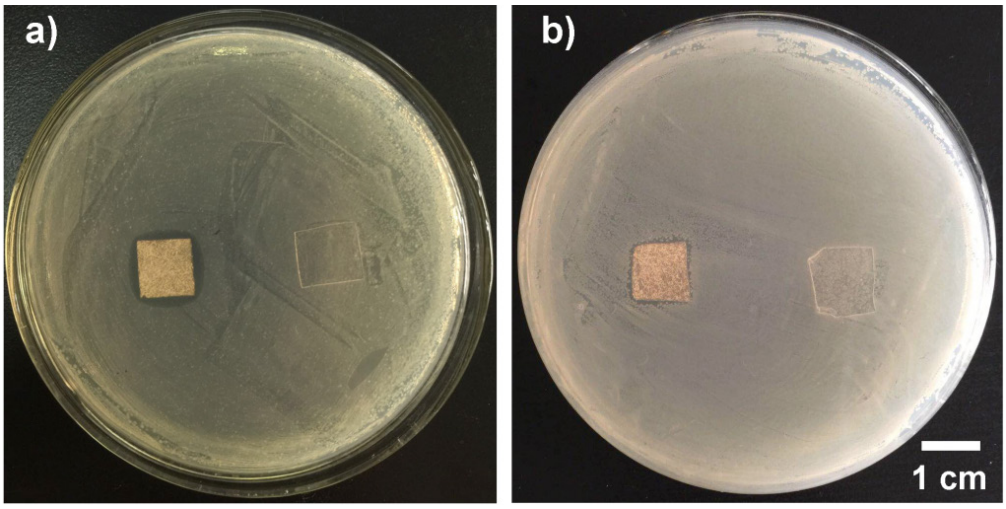

Fig. 6. Photographs of LB plates containing the Ca-ALG/Ag (left side of the dish) and Ca-ALG (right side of the dish) hydrogel film after 24 h of incubation: a) cultures of *Escherichia coli*, b) cultures of *Staphylococcus aureus*.

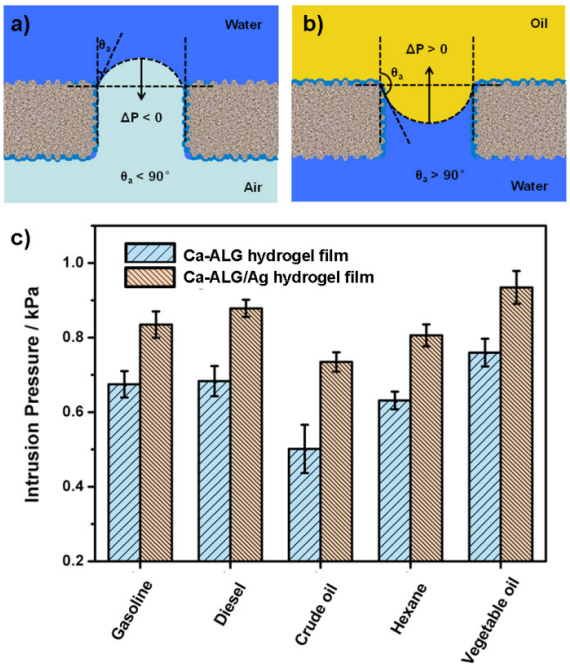

Fig. 7. Schematic illustration of wetting modes and studies of intrusion pressure of the Ca-ALG/Ag hydrogel film. a) When contacted with water, the film cannot sustain any pressure of water ($\Delta P < 0$), thus water can permeate the film spontaneously; b) When contacted with oil, the film can support a certain oil pressure ($\Delta P > 0$). Oil cannot flow through the film below the intrusion pressure. c) Experimental values of intrusion pressures for different oils (The pore size of the film is 95.2 ± 21.7 μm). The Ca-ALG/Ag hydrogel film shows higher intrusion pressures than Ca-ALG hydrogel film, because of the rougher structures.

experiments further proved the antibacterial properties of the Ca-ALG/Ag hydrogel film.

To better understand the process of oil/water separation, we modeled the water and oil wetting processes of the Ca-ALG/Ag hydrogel film in Fig. 7. In theory, an intrusion pressure has to be conquered before the liquid can wet the pore bottom since the advancing contact angle θ_A has to be exceeded, which can be described by the Laplace law as follows [43]:

$$\Delta P = \frac{2\gamma}{R} = -\frac{l\gamma(\cos\theta_A)}{A} \tag{3}$$

where γ is the surface tension; l is the pore's perimeter; R is the meniscus's radius; A is the pore's area; θ_A is the advancing contact angle on the film. The as-prepared Ca-ALG/Ag hydrogel film is superhydrophilic, which means $\theta_A < 90°$ (nearly 0°) and $\Delta P < 0$, thus the film cannot support any water pressure (Fig. 7a). When the water contacts with the film, it will penetrate the film spontaneously because of gravity. Before the separation process, the Ca-ALG/Ag hydrogel film was firstly wetted by water to its balance state. When the oils contact with the film, water will be trapped in the hierarchical rough structures. The underwater superoleophobicity is achieved in such oil/water/solid three-phase system. In this case, $\theta_A > 90°$ (greater than 150°), $\Delta P > 0$, thus the film can support certain oil pressure (Fig. 7b).

Intrusion pressure is the maximum oil pressure that the film can support, which is provided by the weight of oil. Thus the experimental values of intrusion pressures were obtained according to the following equation:

$$P_{exp} = \rho g h_{max} \tag{4}$$

where ρ is the density of the oil, g is acceleration of gravity, h_{max} is the maximum height of oil the film can support. The intrusion pressures of the Ca-ALG/Ag and the Ca-ALG hydrogel films were measured from 10 repeated experiments for a series of oils (Fig. 7c). The Ca-ALG/Ag hydrogel film shows higher intrusion pressures than the Ca-ALG hydrogel film, because the roughness of Ca-ALG/Ag (r = 1.38) is larger than Ca-ALG (r = 1.09). The theoretical intrusion pressures (See details in Supporting Information Fig. S8) were also calculated. It can be seen that the theoretical intrusion pressures are

obviously lower than the experimental values. That is because the theoretical intrusion pressure is calculated based on the hypothesis that the surface of the films are absolutely smooth expect for the micrometer scale pores [39,44]. In fact, the surfaces of Ca-ALG/Ag and Ca-ALG hydrogel films are both rough, especially, the Ca-ALG/Ag hydrogel film which owns much rougher surface. As discussed above, water trapped among these rough structures helps to increase the intrusion pressure. As a result, the experimental intrusion pressures of the Ca-ALG/Ag hydrogel film are larger than the Ca-ALG hydrogel film; the obtained experimental intrusion pressures are larger than theoretical values. From the above, it is clear that the superhydrophilicity allows the water permeate the film while underwater superoleophobicity retains the oil on the film, therefore, oil/water mixture can be separated successfully on such superhydrophilic and underwater superoleophobic film.

4. Conclusions

In summary, we fabricated a porous Ca-ALG/Ag hydrogel film with superhydrophilic and underwater superoleophobic properties, through a novel and eco-friendly "soluble salt-template method". The as-prepared film is stable in complex solution environments, thus can separate oil/water mixtures in highly acidic, alkaline, and salty environments effectively. The introduction of Ag nanoparticles not only enhances the superoleophobicity, but also provides antibacterial activities against *Escherichia coli* (Gram negative bacterium) and *Staphylococcus aureus* (Gram positive bacterium). The Ca-ALG/Ag hydrogel film is stable, biodegradable, and reusable. The multifunctional film has a wide range of applications including the cleanup of marine oil spills and treatment of complicated oily wastewater. Furthermore, other hydrogel films with macro-porous structures can be prepared by this "soluble salt-template method", which enriches the preparation methods of separation materials.

Supporting information

SEM images with different pore size, EDS images, sliding angle image, dynamic underwater oil-adhesion text, cross-sectional SEM image, the study of the roughness, colony counting method and the theoretical values of intrusion pressures (PDF).

Acknowledgment

We are grateful to the financial support from National Natural Science Foundation of China (21501087, 51773086), Major Program of Shandong Province Natural Science Foundation (ZR2018MB039, ZR2018ZC0946), Natural Science Foundation of Shandong Province (ZR2015PC008) and Ph.D. Programs Foundation of Ludong University (LY2015009, LY2015011). We are grateful for crude oil supply from China Petroleum and Petrochemical Research Institute

References

[1] M.A. Shannon, P.W. Bohn, M. Elimelech, J.G. Georgiadis, B.J. Marinas, A.M. Mayes, Science and technology for water purification in the coming decades, Nature, 452 (2008) 301–310.
[2] J.K. Yuan, X.G. Liu, O. Akbulut, J.Q. Hu, S.L. Suib, J. Kong, F. Stellacci, Superwetting nanowire membranes for selective absorption, Nat. Nanotechnol., 3 (2008) 332–336.
[3] V. Singh, M.K. Purkait, C. Das, Cross-flow microfiltration of industrial oily wastewater: experimental and theoretical consideration, Separ. Sci. Technol., 46 (2011) 1213–1223.
[4] S.B. Joye, Deepwater horizon, five years on, Science, 349 (2015) 592–593.
[5] M. Schrope, Oil spill: deep wounds, Nature, 472 (2011) 152.
[6] T.L. Sun, L. Feng, X.F. Gao, L. Jiang, Bioinspired surfaces with special wettability, Accounts Chem. Res., 38 (2005) 644–652.
[7] Z.X. Xue, Y.Z. Cao, N. Liu, L. Feng, L. Jiang, Special wettable materials for oil/water separation, J. Mater. Chem. A, 2 (2014) 2445–2460.
[8] W.F. Zhang, N. Liu, Y.Z. Cao, X. Lin, Y.N. Liu, L. Feng, Superwetting porous materials for wastewater treatment: from immiscible oil/water mixture to emulsion separation, Adv. Mater. Inter., 4 (2017) 1700029.
[9] Q.L. Ma, H.F. Cheng, A.G. Fane, R. Wang, H. Zhang, Recent development of advanced materials with special wettability for selective oil/water separation, Small, 12 (2016) 2186–2202.
[10] L. Feng, Z.Y. Zhang, Z.H. Mai, Y.M. Ma, B.Q. Liu, L. Jiang, D.B. Zhu, A super-hydrophobic and super-oleophilic coating mesh film for the separation of oil and water, Angew Chem. Int. Edit., 43 (2004) 2012–2014.
[11] L. Du, X. Quan, X. Fan, S. Chen, H. Yu, Electro-responsive carbon membranes with reversible superhydrophobicity/superhydrophilicity switch for efficient oil/water separation, Separ. Sci. Technol., 210 (2019) 891–899.
[12] M. Khosravi, S. Azizian, Preparation of superhydrophobic and superoleophilic nanostructured layer on steel mesh for oil-water separation, Separ. Sci. Technol., 172 (2017) 366–373.
[13] J.C. Zou, X.Y. Liu, W.B. Chai, X.Y. Zhang, B.B. Li, Y.X. Wang, Y.N. Ma, Sorption of oil from simulated seawater by fatty acid-modified pomelo peel, Desal. Water Treat., 56 (2015) 939–946.
[14] J. Ge, H.Y. Zhao, H.W. Zhu, J. Huang, L.A. Shi, S.H. Yu, Advanced sorbents for oil-spill cleanup: recent advances and future perspectives, Adv. Mater., 28 (2016) 10459–10490.
[15] M.J. Liu, S.T. Wang, Z.X. Wei, Y.L. Song, L. Jiang, Bioinspired design of a superoleophobic and low adhesive water/solid interface, Adv. Mater., 21 (2009) 665–669.
[16] L. Lin, M.J. Liu, L. Chen, P.P. Chen, J. Ma, D. Han, L. Jiang, Bio-inspired hierarchical macromolecule-nanoclay hydrogels for robust underwater superoleophobicity, Adv. Mater., 22 (2010) 4826–4830.
[17] Z.X. Xue, S.T. Wang, L. Lin, L. Chen, M.J. Liu, L. Feng, L. Jiang, A novel superhydrophilic and underwater superoleophobic hydrogel-coated mesh for oil/water separation, Adv. Mater., 23 (2011) 4270–4273.
[18] M. Obaid, E. Yang, D.H. Kang, M.H. Yoon, I.S. Kim, Underwater superoleophobic modified polysulfone electrospun membrane with efficient antifouling for ultrafast gravitational oil-water separation, Separ. Sci. Technol., 200 (2018) 284–293.
[19] Y.B. Peng, G. Wen, X.L. Gou, Z.G. Guo, Bioinspired fish-scale-like stainless steel surfaces with robust underwater anti-crude-oil-fouling and self-cleaning properties, Separ. Sci. Technol., 202 (2018) 111–118.
[20] T. Yan, H.W. Meng, W.J.H. Hu, F.P. Jiao, Superhydrophilicity and underwater superoleophobicity graphene oxide-micro crystalline cellulose complex-based mesh applied for efficient oil/water separation, Desal. Water Treat., 111 (2018) 155–164.
[21] X.Y. Zhang, C.Q. Wang, X.Y. Liu, J.H. Wang, C.Y. Zhang, Y.L. Wen, PVA/SiO_2-coated stainless steel mesh with superhydrophilic-underwater superoleophobic for efficient oil-water separation, Desal. Water Treat., 126 (2018) 157–163.

[22] S.Y. Zhang, F. Lu, L. Tao, N. Liu, C.R. Gao, L. Feng, Y. Wei, Bio-inspired anti-oil-fouling chitosan-coated mesh for oil/water separation suitable for broad pH range and hyper-saline environments, Acs Appli. Mater. Inter., 5 (2013) 11971–11976.
[23] Y. Cai, Q.H. Lu, X.L. Guo, S.T. Wang, J.L. Qiao, L. Jiang, Salt-tolerant superoleophobicity on alginate gel surfaces inspired by seaweed (Saccharina japonica), Adv. Mater., 27 (2015) 4162–4168.
[24] T. Matsubayashi, M. Tenjimbayashi, M. Komine, K. Manabe, S. Shiratori, Bioinspired hydrogel-coated mesh with superhydrophilicity and underwater superoleophobicity for efficient and ultrafast oil/water separation in harsh environments, Ind. Eng. Chem. Res., 56 (2017) 7080–7085.
[25] J. Yang, Y.F. Xia, P. Xu, B.B. Chen, Super-elastic and highly hydrophobic/superoleophilic sodium alginate/cellulose aerogel for oil/water separation, Cellulose, 25 (2018) 3533–3544.
[26] L.P. Xu, D. Han, X.W. Wu, Q.Q. Zhang, X.J. Zhang, S.T. Wang, A green route for substrate-independent oil-repellent coatings, Sci. Rep., 6 (2016) 38016.
[27] Y.Q. Li, H. Zhang, M.Z. Fan, P.T. Zheng, J.D. Zhuang, L.H. Chen, A robust salt-tolerant superoleophobic alginate/graphene oxide aerogel for efficient oil/water separation in marine environments, Sci. Rep., 7 (2017) 46379.
[28] D. Kolodynska, D. Fila, Lanthanides and heavy metals sorption on alginates as effective sorption materials, Desal. Water Treat., 131 (2018) 238–251.
[29] S.M.A. Soliman, A.M. Ali, M.W. Sabaa, Alginate-based hydrogel for water treatment, Desal. Water Treat., 94 (2017) 129–136.
[30] S. Thakur, B. Sharma, A. Verma, J. Chaudhary, S. Tamulevicius, V.K. Thakur, Recent progress in sodium alginate based sustainable hydrogels for environmental applications, J. Clean. Prod., 198 (2018) 143–159.
[31] Y. Li, H. Zhang, M. Fan, J. Zhuang, L. Chen, A robust salt-tolerant superoleophobic aerogel inspired by seaweedfor efficient oil-water separation in marine environments, Phys. Chem. Chem. Phys., 18 (2016) 25394–25400.
[32] V. Gopishetty, Y. Roiter, I. Tokarev, S. Minko, Multiresponsive biopolyelectrolyte membrane, Adv. Mater., 20 (2008) 4588–4593.
[33] P. Pankongadisak, U.R. Ruktanonchai, P. Supaphol, O. Suwantong, Preparation and characterization of silver nanoparticles-loaded calcium alginate beads embedded in gelatin scaffolds, Aaps Pharmscitech., 15 (2014) 1105–1115.
[34] G.K. Devi, P.S. Kumar, K.S. Kumar, Green synthesis of novel silver nanocomposite hydrogel based on sodium alginate as an efficient biosorbent for the dye wastewater treatment: prediction of isotherm and kinetic parameters, Desal. Water Treat., 57 (2016) 27686–27699.
[35] K.S. Chow, E. Khor, Novel fabrication of open-pore chitin matrixes, Biomacromolecules, 1 (2000) 61–67.
[36] X.Z. And, E. Ruckenstein, Control of pore sizes in macroporous chitosan and chitin membranes, Ind. Eng. Chem. Res., 35 (1996) 4169–4175.
[37] J. Manna, S. Goswami, N. Shilpa, N. Sahu, R.K. Rana, Biomimetic method to assemble nanostructured Ag@ZnO on cotton fabrics: Application as self-cleaning flexible materials with visible-light photocatalysis and antibacterial activities, Acs Appl. Mater. Inter., 7 (2015) 8076–8082.
[38] R.J. Qu, J.J. Gao, B. Tang, Q.L. Ma, B.H. Qu, C.M. Sun, Preparation and property of polyurethane/nanosilver complex fibers, Appl. Surf. Sci., 294 (2014) 81–88.
[39] A. Lafuma, D. Quéré, Superhydrophobic states, Nat. Mater., 2 (2003) 457–460.
[40] Z.X. Xue, M.J. Liu, L. Jiang, Recent developments in polymeric superoleophobic surfaces, J. Polym. Sci. Pol. Phys., 50 (2012) 1209–1224.
[41] E.S. Zhang, Z.J. Cheng, T. Lv, Y.H. Qian, Y.Y. Liu, Anti-corrosive hierarchical structured copper mesh film with superhydrophilicity and underwater low adhesive superoleophobicity for highly efficient oil-water separation, J. Mater. Chem. A, 3 (2015) 13411–13417.
[42] U.K. Fatema, M.M. Rahman, M.R. Islam, M.Y.A. Mollah, M. Susan, Silver/poly(vinyl alcohol) nanocomposite film prepared using water in oil microemulsion for antibacterial applications, J. Colloid Interface Sci., 514 (2018) 648–655.
[43] J.P. Youngblood, T.J. Mccarthy, Ultrahydrophobic polymer surfaces prepared by simultaneous ablation of polypropylene and sputtering of poly(tetrafluoroethylene) using radio frequency plasma, Macromolecules, 32 (1999) 6800–6806.
[44] C. Journet, S. Moulinet, C. Ybert, S.T. Purcell, L. Bocquet, Contact angle measurements on superhydrophobic carbon nanotube forests: Effect of fluid pressure, Europhys. Lett., 71 (2005) 104–109.

Supporting Information

The study of the roughness of the Ca-ALG and Ca-ALG/Ag hydrogel film

The roughness is the ratio of actual area to apparent area. Through the cross-sectional SEM image of the Ca-ALG and Ca-ALG/Ag hydrogel film, the ratio of actual area to apparent area can be represented by the ratio of circumference of section curve and apparent section length. 10 cross-sectional SEM images were counted. The roughness of the Ca-ALG and Ca-ALG/Ag hydrogel film is approximately 1.38 and 1.09 respectively.

Table S1
Contact angles of water droplets (CA) and 1,2-dichloroethane (OCA) on different surfaces in different systems. The pore size of the film is about 95.2 ± 21.7 μm

Systems surfaces	CA (in air)	OCA (in air)	OCA (in water)
Ca-ALG hydrogel film	< 5°	< 5°	152.2 ± 1.2°
Ca-ALG/Ag hydrogel film	< 5°	< 5°	161.4 ± 1.8°

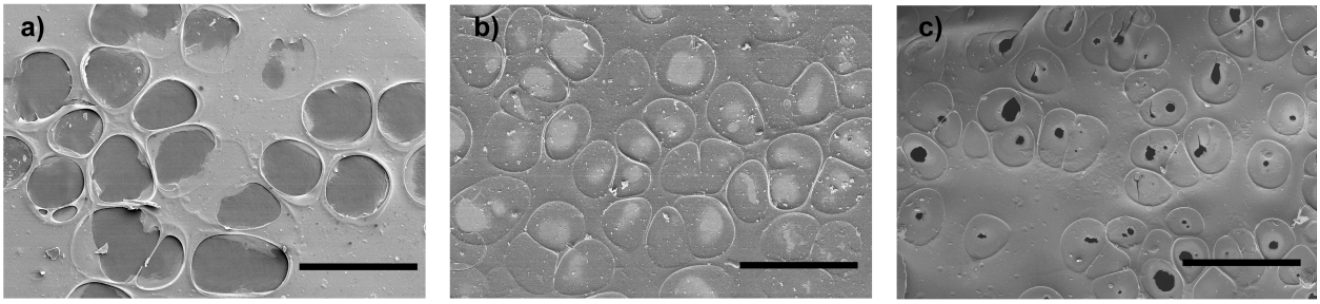

Fig. S1. SEM images of the porous Ca-ALG hydrogel films with different pore size. The pore size are a) 287.9 ± 47.5 μm, b) 95.2 ± 21.7 μm, c) 21.7 ± 10.7 μm, respectively. The scale bar is 500 μm.

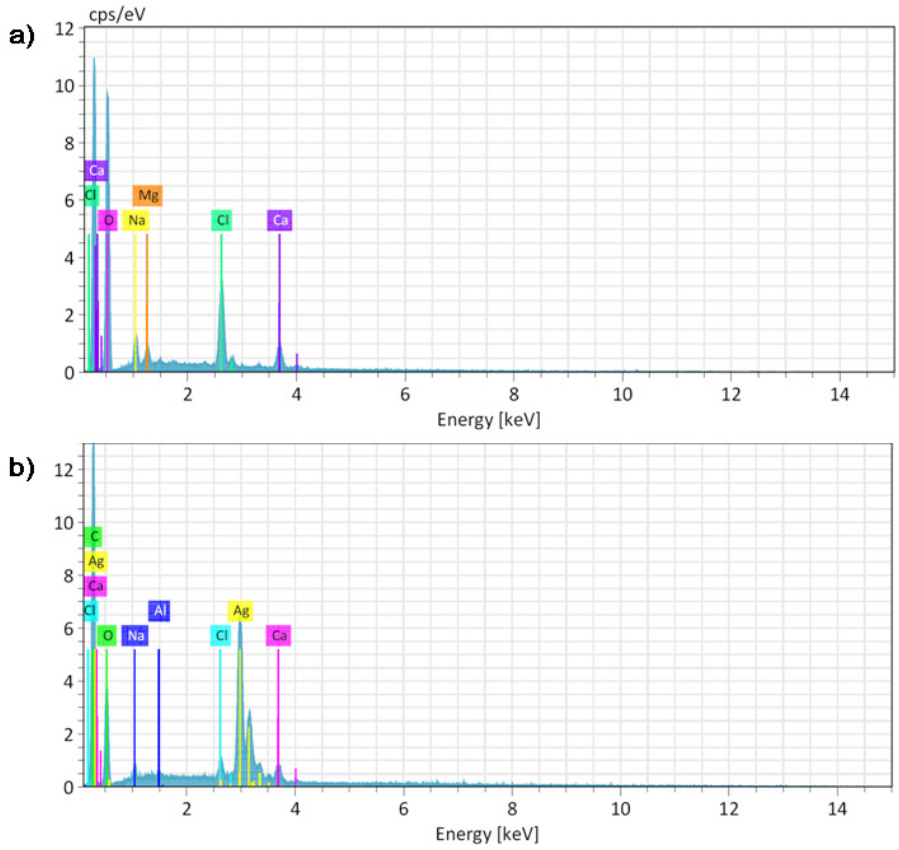

Fig. S2. EDS images of the a) Ca-ALG hydrogel film and b) Ca-ALG/Ag hydrogel film. The presence of Ag can be clearly observed.

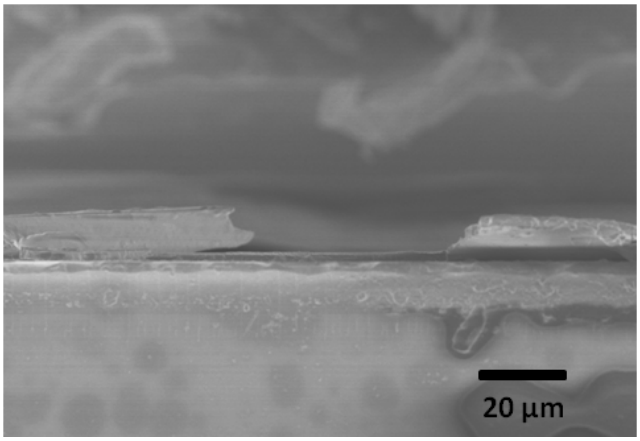

Fig. S3. The cross-sectional SEM image of the Ca-ALG/Ag hydrogel film. The cross section of a pore can be clearly observed.

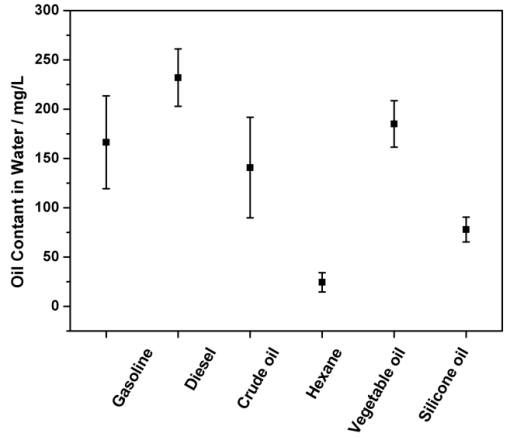

Fig. S6. The oil contents in water after separation.

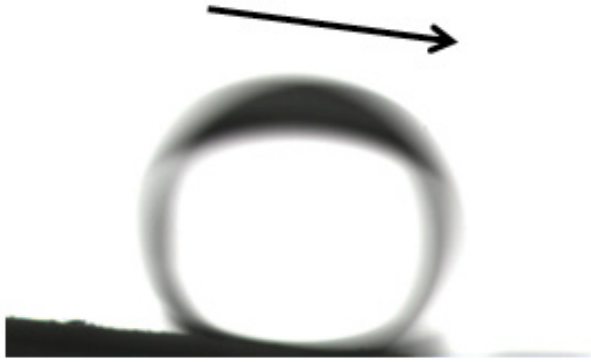

Fig. S4. A typical image of an oil droplet slides away from the surface of the Ca-ALG/Ag hydrogel film (5 µL, 1, 2-dichloroethane).

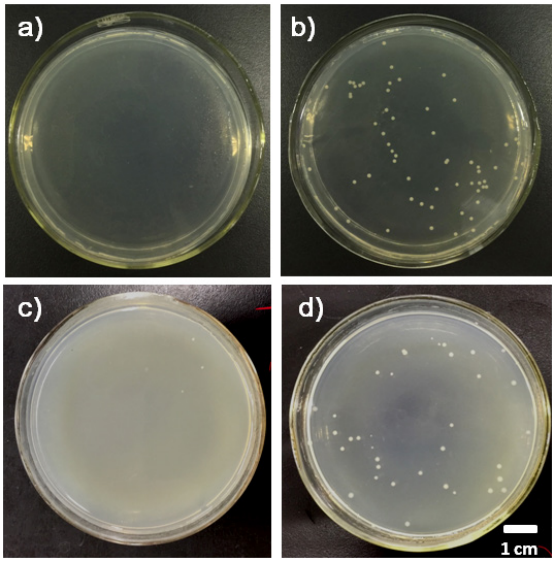

Fig. S7. The colony counting method for the Ca-ALG/Ag hydrogel film against a) *E. coli* and c) *S. aureus*. b) and d) are blank control for *E. coli* (10^{-2}) and *S. aureus* (10^{-1}), respectively.

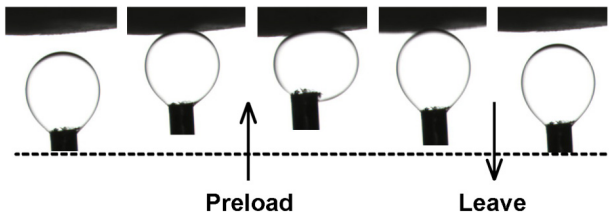

Figure S5. Dynamic underwater oil-adhesion of the Ca-ALG/Ag hydrogel film. An oil droplet (hexane, 3 µL) was used as the detecting probe to contact the surface and then left. The Ca-ALG/Ag hydrogel film exhibits excellent ultra low affinity to the oil droplet. Even the oil droplet was squeezed against the surface with the maximum preload that the system can supply, the Ca-ALG/Ag hydrogel film still showed stable ultra low oil-adhesion property, on which no residual oil can be observed.

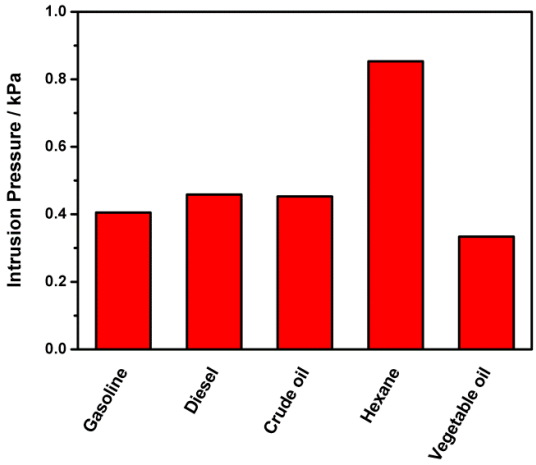

Fig. S8. The theoretical values of intrusion pressure for a series of oils.